

Charge Drive With Active DC Stabilization for Linearization of Piezoelectric Hysteresis

Andrew J. Fleming, *Member, IEEE*

Abstract—Charge drive circuits can significantly reduce piezoelectric nonlinearity; however, they are rarely used in practice because of their limited low-frequency performance, their dependence of voltage gain on the load capacitance, and their requirement for time-consuming tuning procedures. In this report, a new charge drive circuit is proposed that uses a controlled current source with voltage feedback to stabilize the low-frequency behavior. This approach eliminates many of the present difficulties and allows extremely low transition frequencies without a long transient response. Experimental results demonstrate that the proposed charge amplifier can effectively reduce piezoelectric hysteresis and creep to less than 1.3% at scan-rates of 10, 1, and 0.1 Hz.

I. INTRODUCTION

BECAUSE of their high stiffness, compact size, and effectively infinite resolution, piezoelectric actuators are employed in a wide range of industrial, scientific, and commercial applications. Examples include scanning probe microscope positioning systems [1], [2], fuel injection valves [3], and laser beam manipulation [4]. Although piezoelectric actuators have several desirable characteristics, a major disadvantage is the hysteresis exhibited at high electric fields [5], [6]. To avoid positioning errors, many applications require some form of compensation to account for nonlinearity.

The most popular technique for compensation of hysteresis is sensor-based feedback control using integral or proportional-integral (PI) control [7], [8]. Such controllers are simple but are disadvantaged by cost, complexity, limited bandwidth, and sensor-induced noise [9]. In some applications, the requirement for a sensor can be relaxed by self-sensing the position from the actuator current [10], [11]. Alternatively, feedforward approaches use a model to invert nonlinearity [12], [13]. A survey of feedforward and feedback compensation techniques can be found in references [14] and [15].

An alternative technique for reducing hysteresis is to drive the actuator with charge or current rather than voltage [16], [17]. Simply by regulating the current or charge, the hysteresis nonlinearity can be reduced from approximately 10% of the range to 1% [18]–[20]. This technique was originally reported by Comstock in 1981 [17]. Following this work, several variations and improvements ap-

peared; for example, resistive feedback to compensate for drift [18], grounded loads [19], switched capacitor implementation [21], and dynamics compensation [22].

Although the circuit topology of a charge or current amplifier is much the same as a simple voltage amplifier, the uncontrolled nature of the output voltage typically results in the load capacitor being charged. To avoid this problem, a resistive feedback network is commonly employed to stabilize the low-frequency behavior [18]. Unfortunately, this introduces a number of problems:

- the voltage gain is inversely proportional to the load capacitance,
- the dc gain must be tuned to match the ac gain, which can be an extremely slow process,
- the transition frequency is fixed by the component values, and
- transition frequencies below 1 Hz are not practical because of the extremely long transient responses associated with a long time constant.

Because of these practical difficulties, the potential benefits of driving a piezoelectric actuator with charge have been largely ignored in commercial applications. To overcome these difficulties, this article proposes a new method for dc stabilization that utilizes a controlled current source. This method dramatically improves the ease-of-use of a charge drive and has the potential to directly replace a voltage amplifier in many applications.

In the following section, present charge drive circuits are discussed, followed by a description of the active dc stabilization technique. The performance of the active dc stabilization technique is then examined experimentally by driving a standard piezoelectric stack actuator. The key performance characteristics and advantages of active dc stabilization are summarized in the conclusions.

II. EXISTING CHARGE DRIVE CIRCUITS

The schematic diagram of a floating-load charge drive circuit is shown in Fig. 1. The piezoelectric load, modeled as a capacitor C_L and voltage source v_p , is shaded in gray. The high-gain feedback loop works to equate the applied reference voltage V_{in} to the voltage across a sensing capacitor C_s . Neglecting the resistances R_L and R_s , the charge q is

$$q = v_{in}C_s. \quad (1)$$

Manuscript received August 23, 2012; accepted May 3, 2013.

The author is with the Centre for Complex Dynamic Systems and Control, School of Electrical Engineering and Computer Science, University of Newcastle, Callaghan, NSW, Australia (e-mail: Andrew.Fleming@newcastle.edu.au).

DOI <http://dx.doi.org/10.1109/TUFFC.2013.2745>

That is, the gain is C_s coulombs/volt, which implies an input-to-output voltage gain of C_s/C_L V/V.

The foremost problems associated with charge drives are due to stray currents, the finite output impedance, and the dielectric leakage, modeled by R_L . These effects cause the output voltage to drift at low frequencies. However, by setting the ratio of resistances equal to the ratio of capacitances, low-frequency error can be avoided. To maintain a constant voltage gain, the required resistance ratio is

$$\frac{R_L}{R_s} = \frac{C_s}{C_L}. \tag{2}$$

The parallel resistances effectively turn the charge drive into a voltage amplifier below the transition frequency:

$$f_T = \frac{1}{2\pi R_L C_L} \text{ Hz}. \tag{3}$$

Although the parallel resistances act to stabilize the voltage gain at low frequencies, the amplifier now operates as a voltage source below the transition frequency and a charge drive above it. A consequence is that significant reduction of nonlinearity only occurs at frequencies above the transition frequency. Therefore, the transition frequency must be significantly lower than the minimum frequency of operation.

The time constant of the RC network is $1/2\pi f_T$ and the 99% settling time is approximately $5/2\pi f_T$, so a low transition frequency will result in a long transient response after turn-on or a transient event. For example, to operate effectively at 1 Hz, the transition frequency must be 0.1 Hz or less. This results in a time constant of 1.6 s and a 99% settling time of 8 s, which may be impractical for some applications. Therefore, to avoid excessively long transient responses, the minimum operational frequency of a standard charge drive is approximately 1 Hz.

A further inconvenience arises from the fixed nature of the charge gain; the voltage gain of the amplifier is inversely proportional to the load capacitance, which is inconvenient if the load capacitance varies.

III. CHARGE DRIVE WITH ACTIVE DC STABILIZATION

The difficulties encountered with charge drives are primarily due to the method in which the dc gain is controlled. In present designs, the dc gain is controlled by the resistors R_L and R_s . In the following, these resistors are replaced by a controlled current source that regulates the low-frequency voltage gain and eliminates drift. The major benefits of this approach are:

- the low-frequency voltage gain is fixed, rather than a function of load capacitance,
- the resistors for setting the dc gain are eliminated,

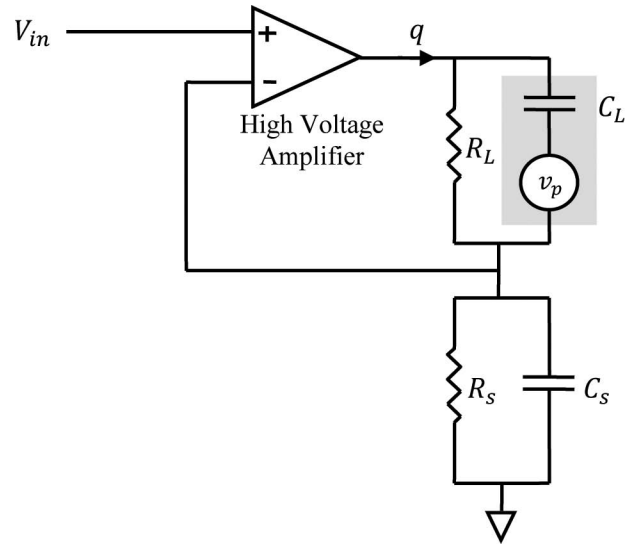


Fig. 1. Simplified schematic diagram of a charge drive [18].

- instead of tuning the dc gain to match the ac gain, which is extremely slow, the ac gain is tuned to match the dc gain, which is fast and straightforward,
- the transition frequency can be varied freely to suit the application, and
- the transition frequency can be extremely low because long transient responses are eliminated.

In Fig. 2, a standard charge source is connected to the piezoelectric load shown in gray. The dc servo loop, shown in blue, consists of a voltage divider $1/\alpha$, a summer, and the current source I_c . The voltage across the load can be computed by superposition. First, neglecting the resistance R_L , the load voltage due to the charge source is

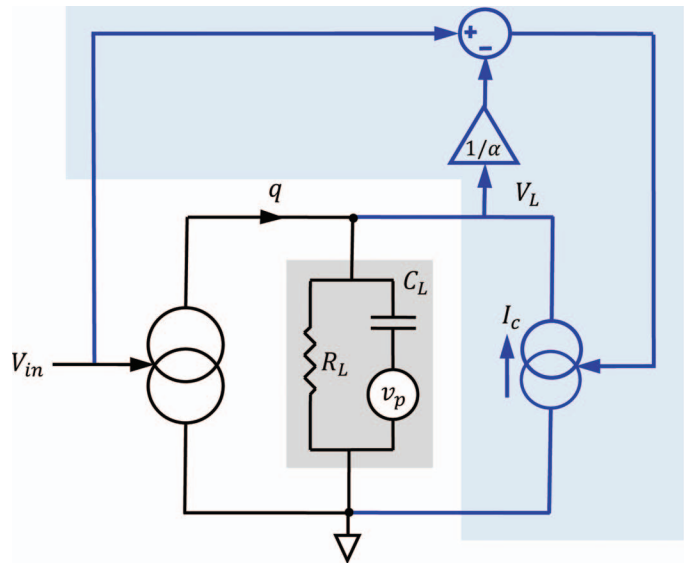


Fig. 2. A charge drive with dc servo control. The dc stabilization loop is shown in blue.

$$V_{Lq} = \frac{C_s}{C_L} V_{in}, \quad (4)$$

where C_s is the gain of the charge source. The second contributor to the load voltage is the current source I_c , which is equal to

$$I_c = k_i \left(V_{in} - \frac{V_L}{\alpha} \right), \quad (5)$$

where k_i is the gain of the current source in amps/volt. By neglecting R_L and applying Ohm's law ($V_L = I_c Z$, where $Z = 1/C_L s$) the voltage due to the current source is

$$V_{Li} = \frac{k_i (V_{in} - V_{Li}/\alpha)}{C_L s}, \quad (6)$$

where k_i is the gain of the current source. Hence, the total load voltage is

$$V_L = \frac{C_s}{C_L} V_{in} + \frac{k_i (V_{in} - V_L/\alpha)}{C_L s}, \quad (7)$$

which is equal to

$$V_L = \frac{C_s}{C_L} V_{in} + \frac{k_i V_{in}}{C_L s} - \frac{k_i V_L}{\alpha C_L s}. \quad (8)$$

Thus,

$$V_L \left(1 + \frac{k_i}{\alpha C_L s} \right) = \frac{C_s}{C_L} V_{in} + \frac{k_i V_{in}}{C_L s}, \quad (9)$$

and

$$V_L = \frac{C_s}{C_L} \frac{1}{\left(1 + \frac{k_i}{\alpha C_L s} \right)} V_{in} + \frac{k_i}{C_L s} \frac{1}{\left(1 + \frac{k_i}{\alpha C_L s} \right)} V_{in}. \quad (10)$$

Therefore, the transfer function from the input to the load voltage is

$$\frac{V_L(s)}{V_{in}(s)} = \frac{C_s}{C_L} \frac{s}{(s + \beta)} + \alpha \frac{\beta}{(s + \beta)}, \quad (11)$$

where $\beta = k_i/\alpha C_L$ is the transition frequency in radians/second. In hertz, the transition frequency is

$$f_T = \frac{k_i}{2\pi\alpha C_L}, \quad (12)$$

which would typically be less than 1 Hz.

The transfer function (11) consists of two parts, one related to the charge source, which is effectively high-pass filtered, and another related to the dc stabilization loop, which acts as a complementary low-pass filter. Because of these complementary filters, the amplifier acts like a charge source above the transition frequency and a voltage amplifier below it (with a gain of α). If the dc gain is fixed,

the charge gain can be adjusted to equal the voltage gain. That is, the charge gain should be such that

$$\frac{C_s}{C_L} = \alpha. \quad (13)$$

If the charge gain is properly adjusted to $C_s = C_L \alpha$, the transfer function is

$$\frac{V_L(s)}{V_{in}(s)} = \alpha \left(\frac{s}{s + \beta} + \frac{\beta}{s + \beta} \right) = \alpha. \quad (14)$$

That is, the voltage gain of the amplifier is α regardless of frequency.

IV. PRACTICAL IMPLEMENTATION

The circuit diagram in Fig. 2 contains a grounded-load charge source and a high-voltage current source, neither of which are straightforward to construct in practice. Although there several methods in which the schematic in Fig. 2 could be implemented, one simple method with desirable characteristics is shown in Fig. 3.

The circuit in Fig. 3 is identical in function to Fig. 2. However, the load is now floating and the current source appears in series rather than in parallel with the load. The advantage of this approach is that the current source is both grounded and exposed only to low voltages. This is significant because a high-voltage current source is difficult to construct with the requisite performance for this application—that is, with low noise, low drift, high impedance, and low offset current.

To allow variation of the charge gain, a gain of $k_q \geq 1$ is incorporated into the charge feedback loop. This decreases the overall charge gain to

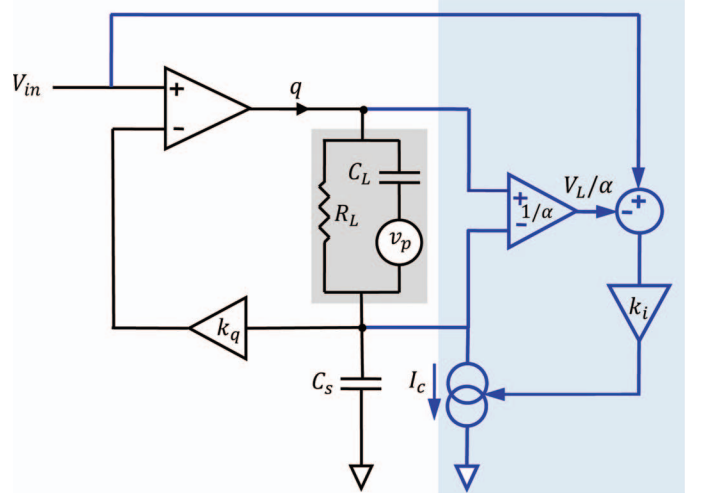


Fig. 3. Practical implementation of a charge drive with dc stabilization circuit (shown in blue).

$$\text{charge gain} = \frac{C_s}{k_q} C/V. \quad (15)$$

The gain k_q also reduces the equivalent voltage gain to $C_s/k_q C_L$. Because k_q only reduces the charge gain, C_s should be designed to provide sufficient gain with the largest expected load capacitance. That is,

$$C_s \geq \alpha C_L. \quad (16)$$

With a smaller load capacitance, k_q can be used to match the dc and ac voltage gain. That is, the equivalent gain is:

$$\frac{C_s}{k_q C_L} = \alpha. \quad (17)$$

V. EXPERIMENTAL RESULTS

The efficacy of the proposed technique is demonstrated by comparing the response of a piezoelectric stack when driven with a standard voltage amplifier and the proposed charge drive. The actuator is a Noliac SCMAP02-10mm multilayer piezoelectric stack actuator (Noliac A/S, Kvistgaard, Denmark) with a full-scale voltage of 60 V, a range of 10.6 μm , and a capacitance of 5.6 μF . The cross-section is 5 \times 5 mm and the length is 10 mm. As shown in Fig. 4, the actuator is mounted horizontally with a polished aluminum cube bonded to the top to provide a suitable sensor target. The capacitive sensor is a Microsense 6810 active probe (Microsense LLC, Lowell, MA) with a sensitivity of 2.5 $\mu\text{m}/\text{V}$, a range of 50 μm , and a stand-off distance of 50 μm .

Because the load capacitance is 5.6 μF , a charge gain of $C_s = 120 \mu\text{C}/\text{V}$ was selected. This provides a maximum voltage gain of 21.4, which is sufficient to achieve the desired voltage gain of $\alpha = 20$. The ac gain of the amplifier was calibrated by applying a 1.25-V (peak) sine-wave with an offset of 1.25 V. The charge gain k_q was adjusted until

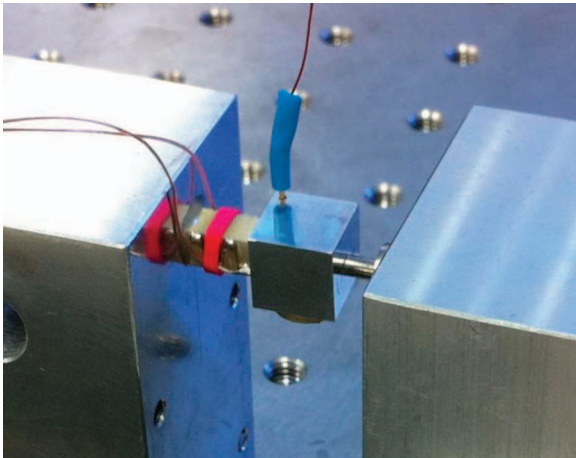


Fig. 4. A horizontally mounted piezoelectric actuator facing a capacitive displacement sensor.

the peak amplitude of the load voltage was equal to the dc value.

A major benefit of the proposed charge drive is that extremely low transition frequencies are possible. To achieve a transition frequency of 7.8 mHz, the required current gain is $k_i = 5.5 \mu\text{A}/\text{V}$. If resistive feedback was used, the resistance values required to obtain a transition frequency of 7.8 mHz would be

$$R_s = \frac{1}{2\pi f_T C_s} = 170 \text{ k}\Omega, \quad \text{and} \quad R_L = 3.40 \text{ M}\Omega.$$

Therefore, with resistive feedback, the time-constant of the RC network is 20.4 s, so the settling time after turn-on or a transient event is more than 100 s, which is not practical. With active dc stabilization, the long settling time can be reduced to less than a second by briefly increasing the current gain from $k_i = 5.5 \mu\text{A}/\text{V}$ to 1 mA/V.

To evaluate the linearity of the charge driven piezoelectric actuator, a 50-V triangular scanning pattern was applied at 10, 1, and 0.1 Hz. The resulting actuator displacements when driven by voltage and charge are plotted in Fig. 5. In this plot, the input signal was normalized to allow a straightforward linearity comparison between the input and displacement.

With a 10 Hz input frequency, the maximum deviation from linear in Fig. 5 is $\pm 1.7\%$ and the rms error is 0.97%. The actuator linearity can also be observed in Fig. 6, where the displacement is plotted against the input voltage and charge. The maximum nonrepeatability in the charge-driven case is 102 nm at 10 Hz (1.2%) versus 840 nm (10.5%) with a voltage amplifier. Although the actuator is not perfectly linearized, the remaining nonlinearity is primarily static. That is, the residual nonlinearity could be inverted by a polynomial, spline, or look-up table.

When the scan speed is reduced to 1 Hz, there is no significant change in performance. At 1 Hz, the maximum deviation from linear was $\pm 1.9\%$ and the rms error was 1.03%. The maximum nonrepeatability in the charge-driven case was 105 nm (1.3%) versus 820 nm (10.2%) for the voltage-driven case.

As discussed in Section II, the lowest practical frequency of operation for a charge amplifier with resistive feedback is approximately 1 Hz. However, because of the low transition frequency of the proposed design, operation at 0.1 Hz and below is feasible without loss of performance. At 0.1 Hz, the maximum deviation from linear was $\pm 1.8\%$ and the RMS error was 1.01%. Furthermore, the maximum nonrepeatability of the charge driven actuator was 83 nm (1.0%) versus 788 nm (9.9%) for a voltage amplifier.

Because of the low frequency of the 0.1-Hz scan, a significant amount of creep is also exhibited by the voltage-driven actuator. The full-scale displacement at 10 Hz is 7.79 μm , whereas at 0.1 Hz, the displacement increases to 8.40 μm , which is an increase of 7.3%. When the actuator is driven by charge, the full-scale displacement only in-

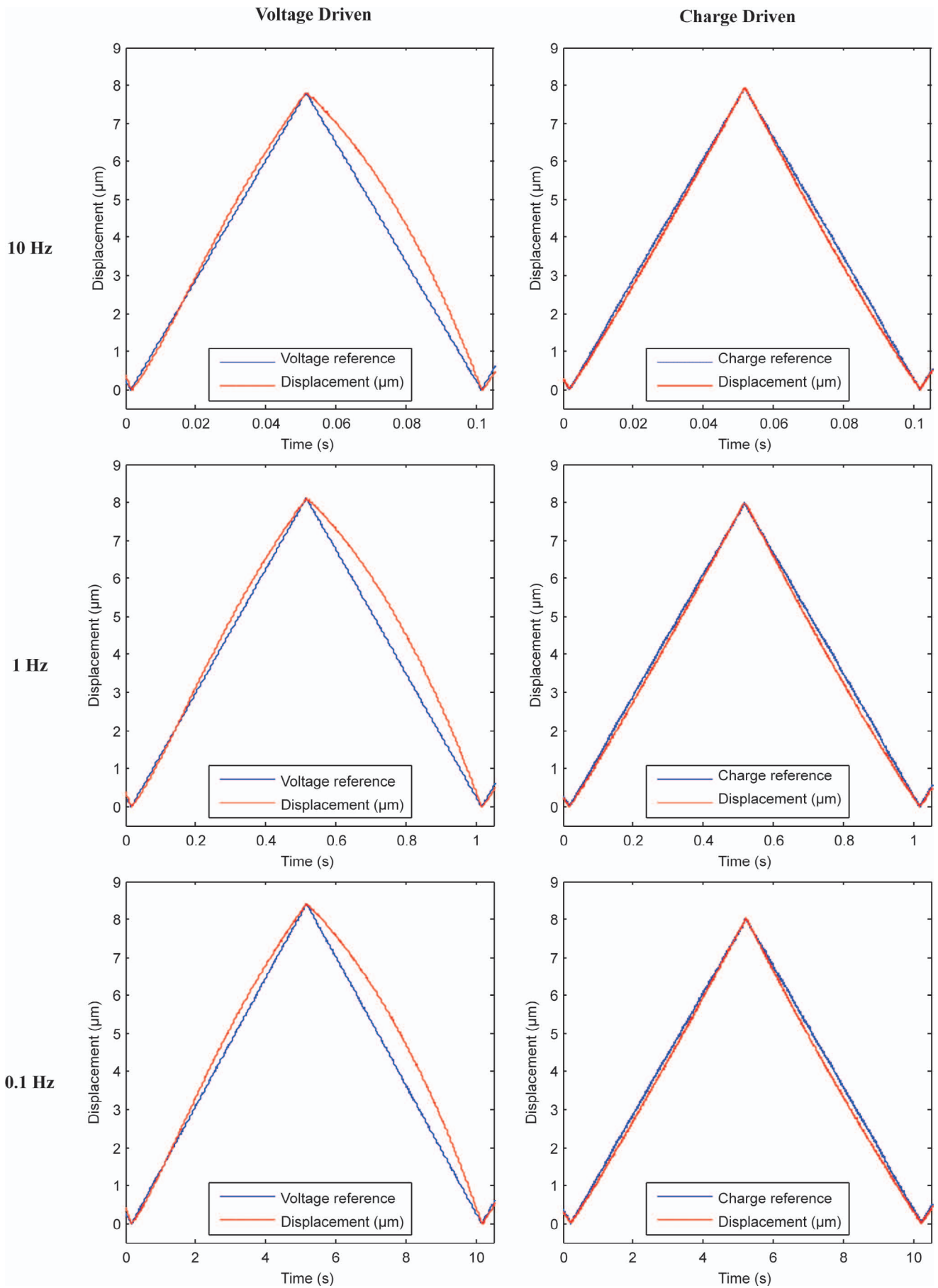


Fig. 5. The displacement resulting from a 50-V triangular scan pattern at 10, 1, and 0.1 Hz.

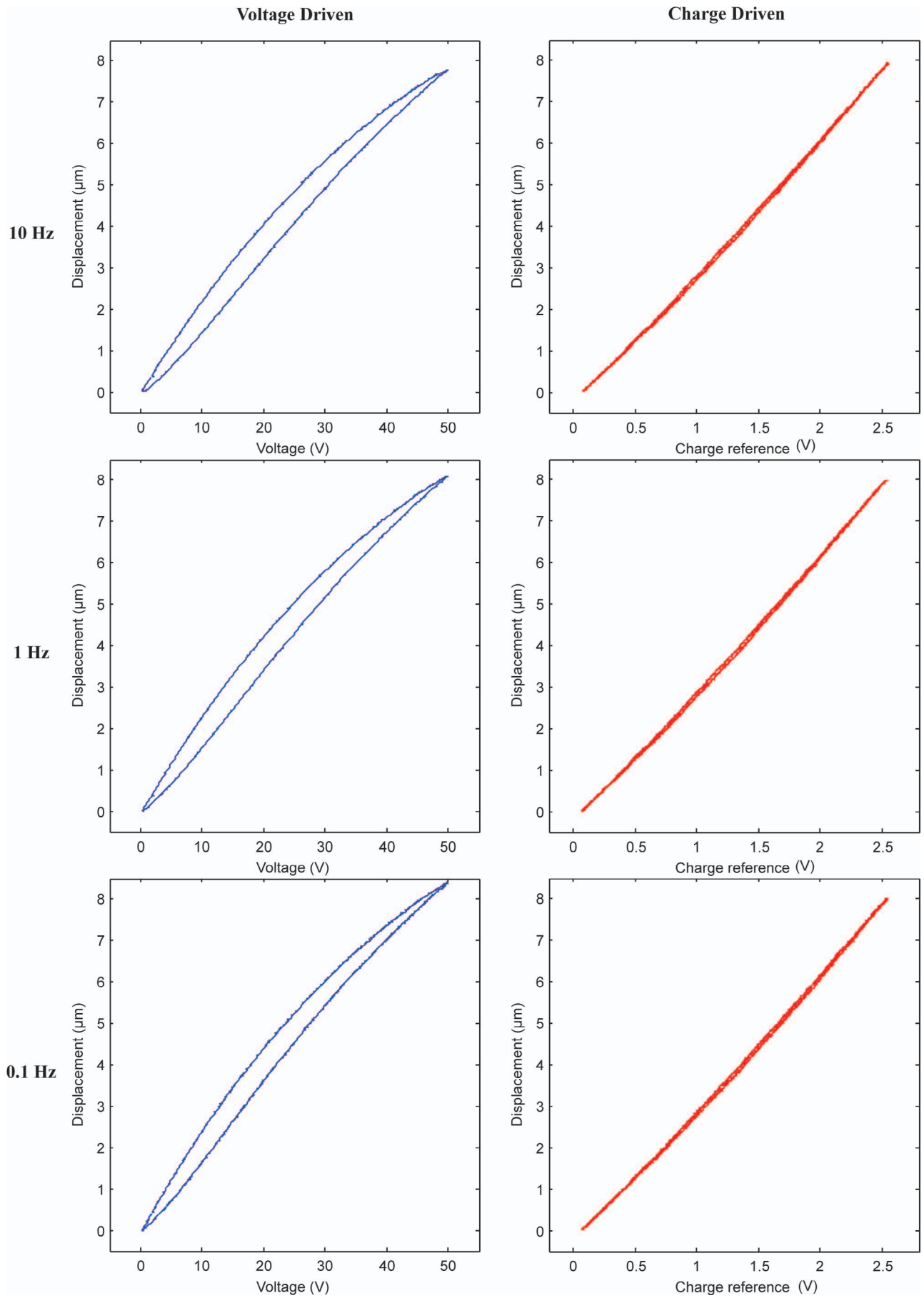


Fig. 6. The displacement versus input charge and voltage for 10, 1, and 0.1 Hz scan rates. 

TABLE I. PRACTICAL COMPARISON OF CHARGE DRIVES (WITH A TRANSITION FREQUENCY OF 0.01 Hz).

Characteristic	Charge drive with resistive feedback	Charge drive with active dc stabilization
Voltage gain	Based on load capacitance	Fixed
DC gain	Must be tuned to ac gain	Fixed
Transition frequency	Inflexible	Variable
AC gain	Inflexible	Variable
Recovery from transients	Slow (e.g., 80 s)	Fast (e.g., 1 s)
Speed of tuning gain	Very slow (minutes)	Fast (seconds)
Offset/bias voltage	Varies with gain	Fixed

creases 1.1% from 7.92 μm to 8.01 μm when the frequency is changed from 10 Hz to 0.1 Hz.

The maximum repeatability error of 1.3% exhibited by the charge driven actuator may eliminate the need for closed-loop control in applications that require accurate periodic motion, such as scanning probe microscopy [20], [23].

VI. CONCLUSIONS

Although charge drives can significantly reduce piezoelectric nonlinearity, they are rarely used because of their limited low-frequency performance, their dependence of voltage gain on the load capacitance, and their requirement for time-consuming tuning procedures.

In contrast to present designs that use resistive feedback, the proposed charge amplifier uses a controlled current source with voltage feedback to stabilize the low-frequency behavior. This approach eliminates many of the present difficulties and allows extremely low transition frequencies without a long transient response. A summary of the improvements is given in Table I.

Experimental results demonstrate that the proposed charge amplifier can effectively reduce piezoelectric hysteresis and creep at 10, 1, and 0.1 Hz in a 60-V piezoelectric stack actuator. The repeatability error, which is the maximum difference between the forward and backward scan paths, is summarized in Table II. At all speeds, the charge drive reduces error to less than 1.3% of the scan range. This is approximately one-ninth the error experienced when using a voltage amplifier. In many applications, such as scanning probe microscopy, a scan error of 1.3% may reduce or eliminate the necessity for closed-loop control. Hence, the use of a charge amplifier could significantly reduce the size, complexity, and cost of piezoelectric positioning systems.

TABLE II. COMPARISON OF REPEATABILITY ERRORS IN VOLTAGE-DRIVEN AND CHARGE-DRIVEN PIEZOELECTRIC ACTUATORS.

Scan speed (Hz)	Repeatability (%)	
	Voltage amplifier	Charge drive
10	10.5	1.2
1	10.2	1.3
0.1	9.9	1.0

REFERENCES

- [1] S. M. Salapaka and M. V. Salapaka, "Scanning probe microscopy," *IEEE Contr. Syst. Mag.*, vol. 28, no. 2, pp. 65–83, Apr. 2008.
- [2] J. A. Butterworth, L. Y. Pao, and D. Y. Abramovitch, "A comparison of control architectures for atomic force microscopes," *Asian J. Control*, vol. 11, no. 2, pp. 175–181, Mar. 2009.
- [3] D. Mehlfeldt, H. Weckenmann, and G. Stöhr, "Modeling of piezoelectrically actuated fuel injectors," *Mechatronics*, vol. 18, no. 5–6, pp. 264–272, 2008.
- [4] S. Z. S. Hassen, M. Heurs, E. H. Huntington, I. R. Petersen, and M. R. James, "Frequency locking of an optical cavity using linear-quadratic Gaussian integral control," *J. Phys. At. Mol. Opt. Phys.*, vol. 42, no. 17, p. 175501 2009.
- [5] S. H. Chang, C. K. Tseng, and H. C. Chien, "An ultra-precision $xy\theta$ piezo-micropositioner. I. Design and analysis," *IEEE Trans. Ultrason. Ferroelectr. Freq. Control*, vol. 46, no. 4, pp. 897–905, Jul. 1999.
- [6] H. Jiang, H. Ji, J. Qiu, and Y. Chen, "A modified Prandtl–Ishlinskii model for modeling asymmetric hysteresis of piezoelectric actuators," *IEEE Trans. Ultrason. Ferroelectr. Freq. Control*, vol. 57, no. 5, pp. 1200–1210, 2010.
- [7] P. Ge and M. Jouaneh, "Tracking control of a piezoceramic actuator," *IEEE Trans. Contr. Syst. Technol.*, vol. 4, no. 3, pp. 209–216, May 1996.
- [8] A. J. Fleming, S. S. Aphale, and S. O. R. Moheimani, "A new method for robust damping and tracking control of scanning probe microscope positioning stages," *IEEE Trans. NanoTechnol.*, vol. 9, no. 4, pp. 438–448, Sep. 2010.
- [9] A. J. Fleming and K. K. Leang, "Integrated strain and force feedback for high performance control of piezoelectric actuators," *Sens. Actuators A*, vol. 161, no. 1–2, pp. 256–265, Jun. 2010.
- [10] A. Badel, J. Qiu, and T. Nakano, "Self-sensing force control of a piezoelectric actuator," *IEEE Trans. Ultrason. Ferroelectr. Freq. Control*, vol. 55, no. 12, pp. 2571–2581, Dec. 2008.
- [11] A. J. Fleming and S. O. R. Moheimani, "Control oriented synthesis of high performance piezoelectric shunt impedances for structural vibration control," *IEEE Trans. Contr. Syst. Technol.*, vol. 13, no. 1, pp. 98–112, Jan. 2005.
- [12] A. A. Eielson, J. T. Gravidahl, and K. Y. Pettersen, "Adaptive feedforward hysteresis compensation for piezoelectric actuators," *Rev. Sci. Instrum.*, vol. 83, no. 8, art. no. 085001, 2012.
- [13] Y. Wu and Q. Zou, "Iterative control approach to compensate for both the hysteresis and the dynamics effects of piezo actuators," *IEEE Trans. Contr. Syst. Technol.*, vol. 15, no. 5, pp. 936–944, Sep. 2007.
- [14] K. K. Leang, Q. Zou, and S. Devasia, "Feedforward control of piezoactuators in atomic force microscope systems," *IEEE Control Syst. Mag.*, vol. 29, no. 1, pp. 70–82, Feb. 2009.
- [15] S. Devasia, E. Eleftheriou, and S. O. R. Moheimani, "A survey of control issues in nanopositioning," *IEEE Trans. Contr. Syst. Technol.*, vol. 15, no. 5, pp. 802–823, Sep. 2007.
- [16] C. V. Newcomb and I. Flinn, "Improving the linearity of piezoelectric ceramic actuators," *IEE Electron. Lett.*, vol. 18, no. 11, pp. 442–443, May 1982.
- [17] R. Comstock, "Charge control of piezoelectric actuators to reduce hysteresis effects," U.S. Patent 4263527, Apr. 21, 1981.
- [18] K. A. Yi and R. J. Veillette, "A charge controller for linear operation of a piezoelectric stack actuator," *IEEE Trans. Contr. Syst. Technol.*, vol. 13, no. 4, pp. 517–526, Jul. 2005.
- [19] A. J. Fleming and S. O. R. Moheimani, "Sensorless vibration suppression and scan compensation for piezoelectric tube nanoposition-

- ers," *IEEE Trans. Contr. Syst. Technol.*, vol. 14, no. 1, pp. 33–44, Jan. 2006.
- [20] A. J. Fleming and K. K. Leang, "Charge drives for scanning probe microscope positioning stages," *Ultramicroscopy*, vol. 108, no. 12, pp. 1551–1557, Nov. 2008.
- [21] L. Huang, Y. T. Ma, Z. H. Feng, and F. R. Kong, "Switched capacitor charge pump reduces hysteresis of piezoelectric actuators over a large frequency range," *Rev. Sci. Instrum.*, vol. 81, no. 9, art. no. 094701, 2010.
- [22] G. M. Clayton, S. Tien, S. Devasia, A. J. Fleming, and S. O. R. Moheimani, "Inverse-feedforward of charge controlled piezopositioners," *Mechatronics*, vol. 18, no. 5–6, pp. 273–281, Jun. 2008.
- [23] A. J. Fleming, "Quantitative SPM topographies by charge linearization of the vertical actuator," *Rev. Sci. Instrum.*, vol. 81, no. 10, art. no. 103701, Oct. 2010.



Andrew J. Fleming graduated from The University of Newcastle, Australia (Callaghan campus) with a Bachelor of Electrical Engineering degree in 2000 and Ph.D. degree in 2004. Dr. Fleming is a Senior Lecturer and Australian Research Council fellow at the School of Electrical Engineering and Computer Science, The University of Newcastle, Australia. His research includes nano-positioning, high-speed scanning probe microscopy, nanofabrication, and micro-cantilever sensors. Dr. Fleming's research awards include the

IEEE Transactions on Control Systems Technology Outstanding Paper Award, The Australian Control Conference Best Student Paper Award, The University of Newcastle Researcher of the Year Award, and the Faculty of Engineering and Built Environment Award for Research Excellence. He is the co-author of two books, several patent applications, and more than 100 journal and conference papers.